Shannon Energy Application for Detection of ECG R-peak using Bandpass Filter and Stockwell Transform Methods

Mohd Zubir SUBOH[1,2], Rosmina JAAFAR[1], Nazrul Anuar NAYAN[1], Noor Hasmiza HARUN[2]
[1]*Department of Electrical, Electronic and Systems Engineering, Faculty of Engineering and Built Environment, Universiti Kebangsaan Malaysia, 43600 Malaysia*
[2]*Medical Engineering Technology Section, Universiti Kuala Lumpur, 53100 Malaysia*
rosmina@ukm.edu.my

***Abstract*—Shannon energy-based algorithm has been implemented in peak detection method of various physiological signals including electrocardiogram, which is used to enhance significant peaks for accurate peak detection. Two significant methods of R-peak detection that apply Shannon energy are identified. However, direct comparison cannot be made due to the differences in database used, number of beat analysed, frequency range selected, and signal processing technique applied. This paper aimed to properly evaluate the performance of Shannon energy-based algorithms for R-peak detection on two methods of bandpass filter and Stockwell transform. Simple enveloping technique using moving average filter is proposed, and a threshold is set to localize R-peak at a selected frequency range of 7-15 Hz. Performance of both methods were then evaluated using all 48 data from MIT-BIH Arrhythmia database. Result showed that both methods are equivalently useful in reducing P and T waves interference and produced similar output of Shannon energy envelope. However, Shannon energy application on bandpass filter offered 99.71% sensitivity, 99.80% positive predictivity and 99.52% accuracy, slightly better than that of the Stockwell transform method that only produced 99.65% sensitivity, 99.68% positive predictivity and 99.33% accuracy.**

***Index Terms*—biomedical signal processing, spectral analysis, electrocardiography, detection algorithms, signal processing algorithms.**

I. INTRODUCTION

Electrocardiogram (ECG) segmentation of various peaks and segments remain as a challenging task due to the signal's non-stationary nature and physiological differences among individuals or patients. The most prominent repeating peaks in ECG is QRS complex or R-peak, which represents the depolarization process in the heart ventricles. R-peak detection allows the determination of heart rate and heart rate variability, which is very useful in predicting various types of cardiovascular diseases [1].

There are many algorithms available for R-peak detection and previous studies showed that these algorithms had resulted more to than 99% accuracy. The basic step of most of the algorithms is to highlight the relevant section of the ECG. This is done by applying filter or transformation methods such as, lowpass filter [2-3], derivative filter [4-7], Fourier transform [8], wavelet transform [9-12] and Hilbert transform [13-16]. Energy of the transformed or filtered signal is then calculated to amplify the significant peak and attenuate the low amplitude noise. Shannon energy is commonly used in this situation rather than classical energy since it calculates the local spectrum of an ECG signal and subsequently reduces the effect of P and T waves [17].

Shannon energy-based algorithms used in R-peak detection have been applied on bandpass filter [13], [18-19] and Stockwell transform or s-transform methods [17], [20]. It is used to enhance R-peak before appropriate algorithm or set of rules are applied to locate the peak. The application has produced promising detection rate with at least 99.80% sensitivity, 99.80% positive predictivity and 99.75% accuracy [20]. However, direct comparison on these methods cannot be done since database used, total beat analyzed, QRS frequency range selected, signal processing applied, and performance measurement are different.

In this study, Shannon energy-based algorithm is reproduced on Butterworth bandpass filter and s-transform methods within frequency range of 7 to 15 Hz. An alternative enveloping method using moving average filter is introduced and simple thresholding technique is applied on both methods to localized R-peaks so that they can be equally compared using 48 data from MIT-BIH Arrhythmia Database (MITDB). The methods performance is evaluated in terms of sensitivity, positive predictivity and accuracy.

II. MIT-BIH ARRHYTHMIA DATABASE (MITDB)

MITDB consists of 48 sets of surface ECG recordings from 47 subjects. Each record has around 30 minute duration, with a sampling frequency (fs) of 360 Hz [21]. Each recording consists of 2 channels - one modified lead II and one from modified leads of V1, V2, V4 or V5. This database is chosen because it is fully annotated and contains variety of peak morphology with considerable amount of noise and motion artefacts, which enhances robust peak detection. For this study, 30-minute recording of all 48 sets of ECG data from MITDB are used for the purpose of comparing Shannon energy application on two filtering methods.

Annotation of beats for MITDB was made separately for each recording by two cardiologists. Disagreement among them were resolved and consequently produced around 110,000 annotated beats. A few corrections on the annotation had been made from time to time until the year of 2010. The annotation on entire records of MITDB had

This study is supported in part by the research grant from Ministry of Higher Education Malaysia (TRGS/1/2019/UKM/01/4/3).

Digital Object Identifier 10.4316/AECE.2020.03005

covered 16 type of beats. This is shown Table I.

TABLE I. TYPE OF BEATS ANNOTATED IN MITDB

Symbol	Meaning
'·' or N	Normal beat
L	Left bundle branch block beat
R	Right bundle branch block beat
A	Atrial premature beat
a	Aberrated atrial premature beat
J	Nodal (junctional) premature beat
S	Supraventricular premature beat
V	Premature ventricular contraction
F	Fusion of ventricular and normal beat
!	Ventricular flutter wave
e	Atrial escape beat
j	Nodal (junctional) escape beat
E	Ventricular escape beat
P	Paced beat
f	Fusion of paced and normal beat
Q	Unclassifiable beat

These annotated beats can be extracted using WFDB toolbox in MATLAB or Octave [22-23]. This toolbox is a collection of functions for reading, writing, and processing physiologic signals and time series in the formats used by PhysioBank databases. The command to extract all annotation at once or separately (e.g.: Normal beat) for each sample is as the following.

```
AllBeat = rdann(filename,'atr');

Normalbeat = rdann(filename,...
                'atr',[],[],[],'N');
```

Total beat counts for separate beat extraction is slightly difference from the total beat count if it is done at once. It is decided to extract the beat separately in this study for known beat types only. The extracted annotations are then combined and sorted in ascending order.

III. QRS COMPLEX FREQUENCY RANGE

ECG signal originates from a combination of multiple electrical activities of the heart and contains enormous diagnostic information that is valuable to clinical decision making [24]. The heart electrical activities basically generate three main waves of P, QRS complex and T. Each wave has its own frequency components. According to Tereshchenko and Josephson [25], most T-wave lies within zero to 10 Hz range while P-wave lies within 5 to 30 Hz frequencies. QRS complex on the other hand have wider range from 8 to 50 Hz and could exceed above 70 Hz for certain abnormal heart condition. Full spectrum of QRS complex is yet to be explored.

The power vs frequency distribution for the ECG signal with noise and motion artefacts is shown in Figure 1 [26]. QRS complex clearly covers a wide range of frequency compared to P an T waves. Researchers have come out with a variety of ranges for QRS complex within 3 to 40 Hz to detect R-peak. The optimal range is found at 8 - 20 Hz according to a study done in 2010 [27]. The study also showed that the frequency range mostly overlapped from 5 to 15 Hz, where QRS complex is more dominant. However, spectral energy of P and T waves are also distributed at frequency lower than 10 Hz. To minimize the effect of those waves, frequency range of 7 - 15 Hz is chosen for this study.

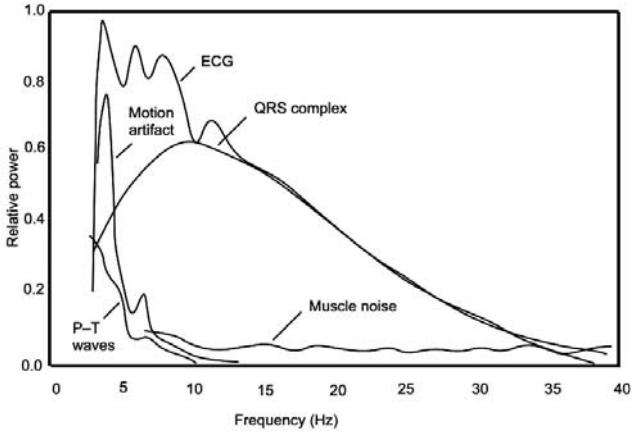

Figure 1. Spectral energy distribution of ECG signal with noise and motion artefact [26]

IV. ECG R-PEAK DETECTION

This study developed a simple peak detection algorithm that applies Shannon energy on two filtering methods of bandpass filter and s-transform at frequency range of 7 – 15 Hz. Moving average filter is used to envelope the energy signal and a threshold is set to localize R-peak. The process is summarized in Figure 2. Direct comparison can be done as exact frequency range and peak finding technique are applied on both methods. Further processing stage to recover missing peak or remove unwanted peak could be different for both methods, hence it is not done in this study.

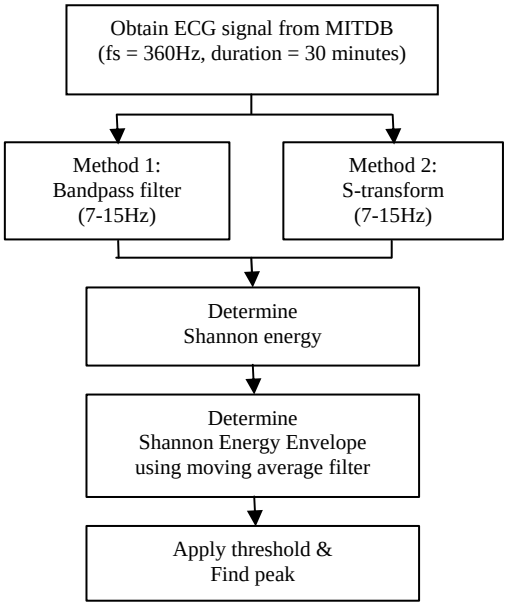

Figure 2. ECG R-peak detection processes

A. Method 1: Shannon energy of bandpass filter (SE-BPF)

Bandpass filter is commonly used as a first step of processing in most R-peak detection algorithms. It reduces the noise, muscle and powerline interferences at high frequency as well as baseline wander, respiration and motion artefact interferences at low frequency. Butterworth bandpass filter (BPF) with cut-off frequencies of 7 and 15 Hz is used in this study. Shannon energy is then calculated using Equation (1), where *x(n)* is the filtered ECG signal.

$$SE(n) = -x(n)^2.\log(x(n)^2) \quad (1)$$

Shannon energy highlights the local spectrum of positive and negative peaks of the filtered ECG signal. These spectrums need to be enveloped to localize R-peak. Various enveloping technique can be used to envelope the QRS complex energies together. In this study, moving average algorithm is proposed as an alternative technique of peak envelope. This technique has the advantageous of removing all small spikes or low amplitude peaks that occur in the Shannon Energy signal. Moving average filter of 140-points is found as the best averaging points for this purpose. Figure 3 shows the proposed envelope technique. The amplitude for both Shannon Energy *(SE)* and Shannon Energy Envelope *(SEE)* are normalized for illustration purpose. R-peak location is then determined when a peak exceeds a defined threshold value set at 10% of the maximum amplitude of Shannon Energy Envelope, *SEE*. Minimum peak distance of 200 ms is used since R-peak could not occur twice within this duration [17].

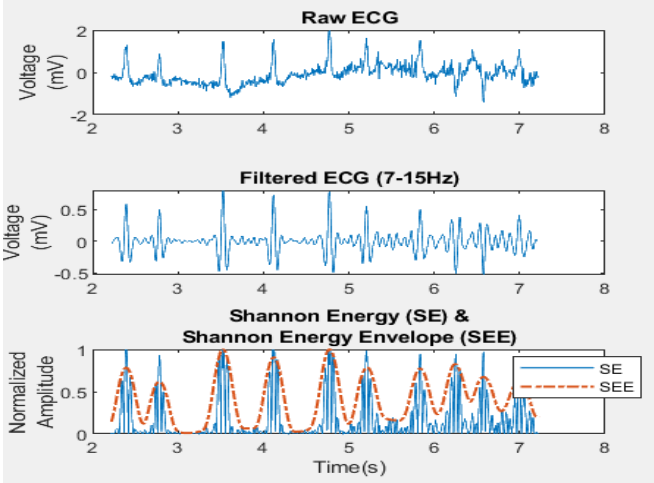

Figure 3. Shannon energy and Shannon energy envelope

B. Method 2: Shannon energy of S-transform (SE-ST)

Another peak enhancing method other than bandpass filter is s-transform. This time-frequency method is quite complex compared to the band pass filter. It is derived from Short-Time Fourier transform (STFT) and Wavelet transform (WT) algorithms, which create frequency dependent resolution while maintaining direct relationship with Fourier spectrum [17]. S-transform of time-varying signal of *x(t)* can be defined as in Equation (2), where *w(t)* is the Gaussian window used to extract the segment of *x(t)*. The discrete form of this equation is presented in Equation (3).

$$S(\tau, f) = \int_{-\infty}^{\infty} x(t).w(t-\tau).e^{-i2\pi ft}dt \quad (2)$$

$$S(j,n) = \sum_{m=0}^{N-1} X(m+n).W(m,n).e^{\frac{i2\pi mj}{N}} \quad (3)$$

The output of s-transform is a M × N matrix, where the row components represent the time while the column components represent the frequency range from 0 to fs/2 Hz. Since output is in time and frequency domain, output of selected frequency range at every time step can be extracted. Hence, s-transform algorithms can be used as a filter to obtain specific range of desired frequency spectrum in time series. Figure 4 shows the effect of s-transform filtering on common frequency ranges used in previous R-peak detection methods. Interference from P and T waves are clearly removed with minimum cut-off frequency of 5 Hz. Narrower shape of spectrum is also found in 7-15 Hz frequency range, which clearly highlights the R-peak.

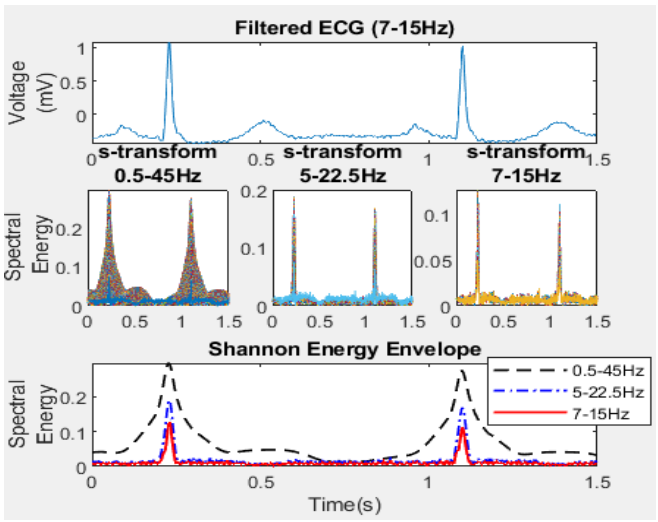

Figure 4. S-transform frequency filtering

S-transform also has the advantage in modifying the ECG spectrum with better frequency or time resolution. This could be done by adjusting the Gaussian window to different length or duration. Shorter window's length is good for time resolution while longer window's length is good for frequency resolution. Figure 5 shows the effect of average frequency spectrum on three different window lengths. Two-second window is chosen for this analysis to localize R-peak since it gives better time resolution. This could reduce the possibility of miss-peak detection since the successive R-peak could occur just after 200 ms. With this setting, Shannon energy is determined as in Equation (4), where *|S(j,n)|* represent the absolute energy of the transformed signal. The exact thresholding and peak finding techniques as in SE-BPF method are then applied.

$$SE(j) = -|S(j,n)|^2.\log|S(j,n)|^2 \quad (4)$$

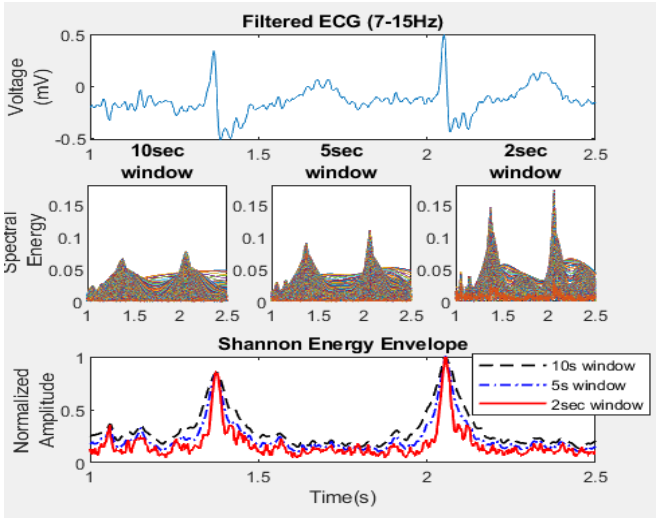

Figure 5. Spectrum effect of s-transform at different window's length

Despite the flexibility of s-transform analysis, the algorithm required high computational power to provide average spectrum of every time step. The computational time is directly proportional to the duration of an ECG signal, which makes it impracticable for real-time application. In order to get fast and accurate spectrum, the ECG signal obtained from MITDB is segmented to 30 samples of 60-second each. Automated peak detection algorithm is developed to detect the R-peak of each sample and result is presented as total for each ECG data.

V. RESULTS

The exact frequency range and peak detection technique are applied on both methods of SE-BPF and SE-ST with the purpose of unbiased comparison. Step by step of the peak finding technique for both methods is shown in Figure 6. All peaks are successfully detected on this example in both methods. Clear main peaks and similar energy envelopes are found on both methods even though there are some interference on the Raw ECG signal between fifth to sixth second.

Detected peak's location might be slightly shifted from the actual peak's location due to filtering and averaging processes. The location of detected peak is compared with location of actual peak. Difference of less than 18-points (50 ms) is used to verify that the detected peak has correct location. This is about half of QRS complex normal duration, which is 80-100 ms [28].

The proposed peak detection methods of SE-BPF and SE-ST are tested on a total of 109744 beats from 48 data of MITDB. Correct peak detected is counted as True Positive (TP), otherwise it is counted as False Positive (FP). If the number of detected peaks is less than the number of actual peaks, then the difference between them are considered as missed peak or False Negative (FN).

Performance can be measured based on the total count of this number in each data. Percentage of sensitivity (Se), positive predictivity (+P), error rate (Er) and accuracy (Acc) for both methods are determined using Equation (5) to Equation (8). Sensitivity refers to the capability of the system to detect all peaks while positive predictivity refers to the ability to detect correct peaks. Both evaluations are important to minimize error on further analysis which could dangerously lead to the triggering of false diagnosis or false alarm. Results are recorded in Table II and Table III for SE-BPF method and SE-ST method, respectively.

$$Se(\%) = TP / (TP + FN).100 \quad (5)$$

$$P(\%) = TP / (TP + FP).100 \quad (6)$$

$$Er(\%) = (FP + FN) / (TotalBeat).100 \quad (7)$$

$$Acc(\%) = TP / (TP + FP + FN).100 \quad (8)$$

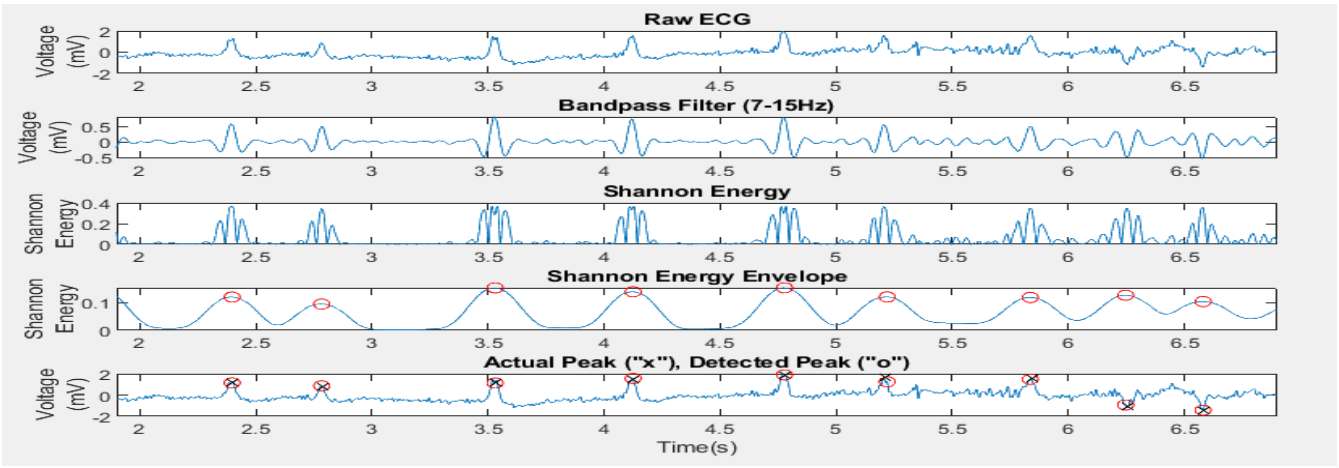

(a) SE-BPF method

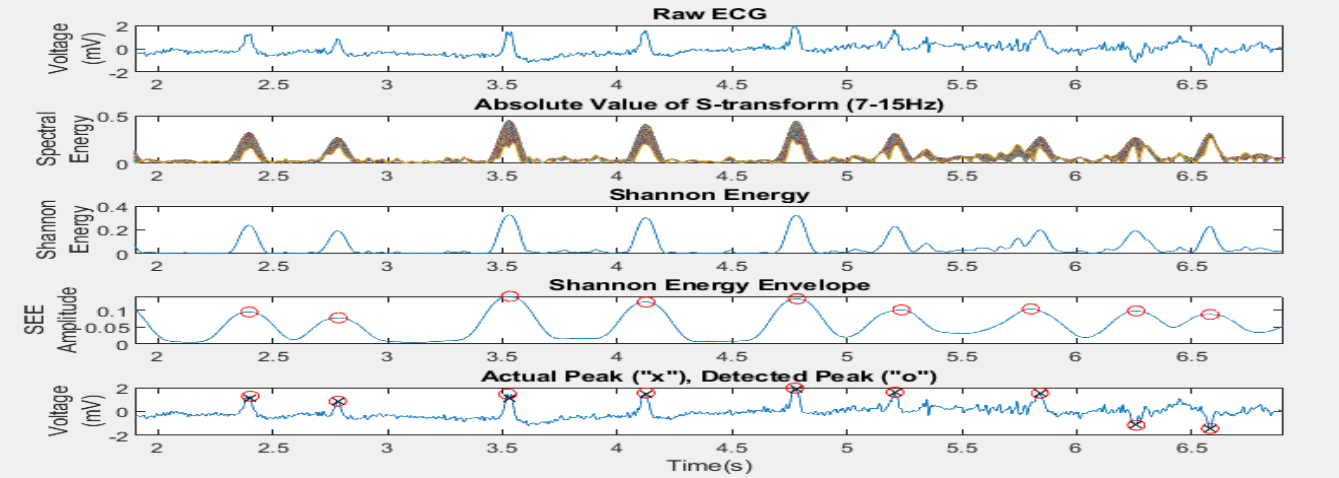

(b) SE-ST method

Figure 6. Peak detection steps for SE-BPF and SE-ST methods

TABLE II. PERFORMANCE OF SE-BPF METHOD

No	Total Beat	Detected Beat	TP	FP	FN	Se (%)	+P (%)	Er (%)	Acc (%)
100	2265	2265	2265	0	0	100.00	100.00	0.00	100.00
101	1864	1863	1861	2	1	99.95	99.89	0.16	99.84
102	2180	2180	2180	0	0	100.00	100.00	0.00	100.00
103	2078	2078	2078	0	0	100.00	100.00	0.00	100.00
104	2222	2225	2219	6	0	100.00	99.73	0.27	99.73
105	2595	2596	2560	36	0	100.00	98.61	1.39	98.61
106	2021	2024	2021	3	0	100.00	99.85	0.15	99.85
107	2131	2131	2130	1	0	100.00	99.95	0.05	99.95
108	1757	1761	1714	47	0	100.00	97.33	2.68	97.33
109	2524	2524	2524	0	0	100.00	100.00	0.00	100.00
111	2118	2118	2116	2	0	100.00	99.91	0.09	99.91
112	2531	2532	2531	1	0	100.00	99.96	0.04	99.96
113	1789	1789	1789	0	0	100.00	100.00	0.00	100.00
114	1873	1872	1872	0	1	99.95	100.00	0.05	99.95
115	1952	1946	1946	0	6	99.69	100.00	0.31	99.69
116	2404	2435	2404	31	0	100.00	98.73	1.29	98.73
117	1530	1530	1530	0	0	100.00	100.00	0.00	100.00
118	2271	2273	2271	2	0	100.00	99.91	0.09	99.91
119	1981	1982	1981	1	0	100.00	99.95	0.05	99.95
121	1856	1856	1855	1	0	100.00	99.95	0.05	99.95
122	2470	2468	2468	0	2	99.92	100.00	0.08	99.92
123	1513	1515	1513	2	0	100.00	99.87	0.13	99.87
124	1613	1614	1613	1	0	100.00	99.94	0.06	99.94
200	2593	2602	2593	9	0	100.00	99.65	0.35	99.65
201	1959	1957	1957	0	2	99.90	100.00	0.10	99.90
202	2130	2127	2127	0	3	99.86	100.00	0.14	99.86
203	2999	2966	2959	7	33	98.90	99.76	1.33	98.67
205	2649	2648	2648	0	1	99.96	100.00	0.04	99.96
207	2322	2088	2079	9	234	89.88	99.57	10.47	89.53
208	2954	2941	2936	5	13	99.56	99.83	0.61	99.39
209	3004	2999	2998	1	5	99.83	99.97	0.20	99.80
210	2643	2640	2636	4	3	99.89	99.85	0.26	99.74
212	2741	2740	2740	0	1	99.96	100.00	0.04	99.96
213	3241	3240	3240	0	1	99.97	100.00	0.03	99.97
214	2259	2257	2256	1	2	99.91	99.96	0.13	99.87
215	3353	3353	3353	0	0	100.00	100.00	0.00	100.00
217	2203	2203	2201	2	0	100.00	99.91	0.09	99.91
219	2147	2148	2147	1	0	100.00	99.95	0.05	99.95
220	2041	2040	2040	0	1	99.95	100.00	0.05	99.95
221	2420	2419	2419	0	1	99.96	100.00	0.04	99.96
222	2474	2472	2465	7	2	99.92	99.72	0.36	99.64
223	2597	2597	2597	0	0	100.00	100.00	0.00	100.00
228	2071	2069	2051	18	2	99.90	99.13	0.97	99.03
230	2249	2251	2248	3	0	100.00	99.87	0.13	99.87
231	1565	1566	1565	1	0	100.00	99.94	0.06	99.94
232	1776	1785	1775	10	0	100.00	99.44	0.56	99.44
233	3071	3068	3068	0	3	99.90	100.00	0.10	99.90
234	2745	2745	2745	0	0	100.00	100.00	0.00	100.00
	109744	**109498**	**109284**	**214**	**317**	**99.71**	**99.80**	**0.48**	**99.52**

TABLE III. PERFORMANCE OF SE-ST METHOD

No	Total Beat	Detected Beat	TP	FP	FN	Se (%)	+P (%)	Er (%)	Acc (%)
100	2265	2265	2265	0	0	100.00	100.00	0.00	100.00
101	1864	1862	1859	3	2	99.89	99.84	0.27	99.73
102	2180	2180	2179	1	0	100.00	99.95	0.05	99.95
103	2078	2078	2077	1	0	100.00	99.95	0.05	99.95
104	2222	2234	2215	19	0	100.00	99.15	0.86	99.15
105	2595	2582	2552	30	13	99.49	98.84	1.66	98.34
106	2021	2017	2014	3	4	99.80	99.85	0.35	99.65
107	2131	2131	2125	6	0	100.00	99.72	0.28	99.72
108	1757	1759	1722	37	0	100.00	97.90	2.11	97.90
109	2524	2523	2521	2	1	99.96	99.92	0.12	99.88
111	2118	2119	2116	3	0	100.00	99.86	0.14	99.86
112	2531	2531	2530	1	0	100.00	99.96	0.04	99.96
113	1789	1789	1787	2	0	100.00	99.89	0.11	99.89
114	1873	1872	1871	1	1	99.95	99.95	0.11	99.89
115	1952	1946	1946	0	6	99.69	100.00	0.31	99.69
116	2404	2388	2385	3	16	99.33	99.87	0.79	99.21
117	1530	1531	1530	1	0	100.00	99.93	0.07	99.93
118	2271	2272	2271	1	0	100.00	99.96	0.04	99.96
119	1981	1977	1977	0	4	99.80	100.00	0.20	99.80
121	1856	1855	1854	1	1	99.95	99.95	0.11	99.89
122	2470	2468	2468	0	2	99.92	100.00	0.08	99.92
123	1513	1511	1511	0	2	99.87	100.00	0.13	99.87
124	1613	1612	1589	23	1	99.94	98.57	1.49	98.51
200	2593	2595	2587	8	0	100.00	99.69	0.31	99.69
201	1959	1950	1948	2	9	99.54	99.90	0.56	99.44
202	2130	2125	2125	0	5	99.77	100.00	0.23	99.77
203	2999	2947	2888	59	52	98.23	98.00	3.70	96.30
205	2649	2642	2641	1	7	99.74	99.96	0.30	99.70
207	2322	2135	2076	59	187	91.74	97.24	10.59	89.41
208	2954	2934	2929	5	20	99.32	99.83	0.85	99.15
209	3004	2997	2996	1	7	99.77	99.97	0.27	99.73
210	2643	2641	2621	20	2	99.92	99.24	0.83	99.17
212	2741	2740	2736	4	1	99.96	99.85	0.18	99.82
213	3241	3241	3240	1	0	100.00	99.97	0.03	99.97
214	2259	2248	2244	4	11	99.51	99.82	0.66	99.34
215	3353	3352	3350	2	1	99.97	99.94	0.09	99.91
217	2203	2200	2195	5	3	99.86	99.77	0.36	99.64
219	2147	2143	2142	1	4	99.81	99.95	0.23	99.77
220	2041	2040	2040	0	1	99.95	100.00	0.05	99.95
221	2420	2416	2416	0	4	99.83	100.00	0.17	99.83
222	2474	2472	2470	2	2	99.92	99.92	0.16	99.84
223	2597	2597	2591	6	0	100.00	99.77	0.23	99.77
228	2071	2071	2048	23	0	100.00	98.89	1.11	98.89
230	2249	2247	2247	0	2	99.91	100.00	0.09	99.91
231	1565	1563	1563	0	2	99.87	100.00	0.13	99.87
232	1776	1781	1771	10	0	100.00	99.44	0.56	99.44
233	3071	3066	3064	2	5	99.84	99.93	0.23	99.77
234	2745	2745	2745	0	0	100.00	100.00	0.00	100.00
	109744	**109390**	**109037**	**353**	**378**	**99.65**	**99.68**	**0.67**	**99.33**

TABLE IV. COMPARISON OF SHANNON ENERGY-BASED ALGORITHMS FOR R-PEAK DETECTION

Author,Year	Database	Method	Total Beat	FN	FP	Se (%)	+P (%)	Er (%)	Acc (%)
Manikandan, 2012 [13]	MITDB	Bandpass filter	109496	79	140	99.93	99.96	0.205	99.79
Zhu, 2013 [18]	MITDB	Bandpass filter	109494	93	91	99.92	99.92	0.168	99.83
Zidelmal, 2014 [17]	MITDB	S-transform	108323	171	97	99.84	99.91	0.25	-
Beyramienanlou, 2017 [19]	*PTB	Bandpass filter	119054	91	93	99.92	99.92	0.155	99.85
Navin, 2019 [20]	MITDB	S-transform	64385	93	72	99.80	99.80	0.25	-
Current study, 2020 Method 1: SE-BPF	**MITDB**	**Bandpass filter**	**109744**	**317**	**214**	**99.71**	**99.80**	**0.48**	**99.52**
Method 2: SE-ST	**MITDB**	**S-transform**	**109744**	**378**	**353**	**99.65**	**99.68**	**0.67**	**99.33**

***PTB = Physikalish-Technische Bundesanstalt Database*

The results in Table II and Table III show that Shannon energy application is really practicable for R-peak detection. Accuracy above 99% are recorded in both SE-BPF and SE-ST methods even though minimal processing steps of peak enhancing, simple enveloping and fixed thresholding are applied. SE-BPF method however had produced slightly better performance in sensitivity, positive predictivity and accuracy compared to SE-SE method. Higher percentage of error (0.67%) in SE-ST method shows higher potential of a peak is not detected or detected at wrong location. The main reason is that SE-ST method is done in 30 separate segmented samples for each MITDB data. The probability for incorrect detection at first and last peak of each sample is quite high, where peak point could be easily shifted during signal filtering, transforming or averaging processes.

Indirect comparison (due to different database and number of samples analysed) among the previous Shannon energy-based algorithms is shown in Table IV. Navin et al [20] had achieved the least positive predictivity of using s-transform method despite the minimal number of beats analysed. Manikandan et al. [13] achieved highest sensitivity and positive predictivity by combining Shannon energy with Hilbert transform algorithm. However, the processing required high memory and had produced delay. Zhu et al. [18] and Beyramienanlou et al. [19] had achieved equally high sensitivity and positive productivity of 99.92% on different methods and databases. This proves that Shannon energy application is very useful and robust in detecting R-peak.

In general, this study has proved the feasibility of Shannon energy application on R-peak detection. Selected frequency range of 7-15 Hz has greatly reduced the interference of P and T waves. Simple enveloping technique proposed in this study using moving average filter, has significantly remove the effect of low amplitude energy on both methods. SE-BPF method is discovered as more accurate and simpler compared to the SE-ST method. However, SE-ST method can also be useful as it provides information in time and frequency domains, despite its computational complexity. Multiple parameters in this method can be manipulated to have variety of output signals in terms of signal filtering and resolution. The overall performance of these methods could be improved by introducing adaptive thresholding or recognizing noise and false peak in further processing stage.

VI. CONCLUSION

The application of Shannon energy in detecting ECG R-peak was tested on two methods of bandpass filter (SE-BPF) and s-transform (SE-ST). Performance of both methods can be directly compared as equal frequency range, processing technique and performance measurement are applied. Both methods gave similar performance in reducing the influence of P and T waves using the proposed frequency range of 7-15 Hz. Despite simpler algorithm used in SE-BPF method, it achieved slightly better performance of 99.71% sensitivity, 99.80% positive predictivity and 99.52% accuracy as compared to the SE-ST method. However, SE-ST method are more flexible in producing desired spectrum in time-frequency domain, but it requires longer computational time and not suitable for real-time application.

REFERENCES

[1] R. McCraty and F. Shaffer, “Heart rate variability: New perspectives on physiological mechanisms, assessment of self-regulatory capacity, and health risk,” Glob. Adv. Heal. Med., vol. 4, no. 1, pp. 46–61, 2015, doi: 10.7453/gahmj.2014.073.

[2] P. Laguna et al., “New algorithm for QT interval analysis in 24-hour Holter ECG: performance and applications,” Med. Biol. Eng. Comput., vol. 28, no. 1, pp. 67–73, 1990, doi: 10.1007/BF02441680.

[3] P. Laguna, R. Jane, and C. Pere, “Automatic detection of wave boundaries in multilead ECG,” Computers and Biomedical Research, vol. 27. pp. 45–60, 1994. doi: 10.1006/cbmr.1994.1006.

[4] B. Frénay, G. De Lannoy, and M. Verleysen, “Emission modelling for supervised ecg segmentation using finite differences,” IFMBE Proc., vol. 22, pp. 1212–1216, 2008, doi: 10.1007/978-3-540-89208-3_290.

[5] G. Schreier, D. Hayn, and S. Lobodzinski, “Development of a New QT Algorithm with Heterogenous ECG Databases,” J. Electrocardiol., vol. 36, no. SUPPL., pp. 145–150, 2003, doi: 10.1016/j.jelectrocard.2003.09.039.

[6] J. A. Vila, Y. Gang, J. M. R. Presedo, M. Fernândez-Delgado, S. Barro, and M. Malik, “A new approach for TU complex characterization,” IEEE Trans. Biomed. Eng., vol. 47, no. 6, pp. 764–772, 2000, doi: 10.1109/10.844227.

[7] R. Gupta, M. Mitra, K. Mondal, and S. Bhowmick, “A derivative-based approach for QT-segment feature extraction in digitized ECG record,” Proc. - 2nd Int. Conf. Emerg. Appl. Inf. Technol. EAIT 2011, pp. 63–66, 2011, doi: 10.1109/EAIT.2011.61.

[8] I. S. N. Murthy and U. C. Niranjan, “Component wave delineation of ECG by filtering in the Fourier domain,” Med. Biol. Eng. Comput., vol. 30, no. 2, pp. 169–176, 1992, doi: 10.1007/BF02446127.

[9] H. Li and X. Wang, “Detection of electrocardiogram characteristic points using lifting wavelet transform and Hilbert transform,” Trans. Inst. Meas. Control, vol. 35, no. 5, pp. 574–582, 2013, doi: 10.1177/0142331212460720.

[10] K. Friganovic, D. Kukolja, A. Jovic, M. Cifrek, and G. Krstacic, "Optimizing the Detection of Characteristic Waves in ECG Based on Processing Methods Combinations," IEEE Access, vol. 6, 2018, doi: 10.1109/ACCESS.2018.2869943.

[11] J. P. Martínez, R. Almeida, S. Olmos, A. P. Rocha, and P. Laguna, "A Wavelet-Based ECG Delineator Evaluation on Standard Databases," IEEE Trans. Biomed. Eng., vol. 51, no. 4, pp. 570–581, 2004, doi: 10.1109/TBME.2003.821031.

[12] J. P. V. Madeiro, P. C. Cortez, J. A. L. Marques, C. R. V. Seisdedos, and C. R. M. R. Sobrinho, "An innovative approach of QRS segmentation based on first-derivative, Hilbert and Wavelet Transforms," Med. Eng. Phys., vol. 34, no. 9, pp. 1236–1246, 2012, doi: 10.1016/j.medengphy.2011.12.011.

[13] M. S. Manikandan and K. P. Soman, "A novel method for detecting R-peaks in electrocardiogram (ECG) signal," Biomed. Signal Process. Control, vol. 7, no. 2, pp. 118–128, 2012, doi: 10.1016/j.bspc.2011.03.004.

[14] R. Kumar, A. Kumar, and G. K. Singh, "Electrocardiogram signal compression based on 2D-transforms: A research overview," J. Med. Imaging Heal. Informatics, vol. 6, no. 2, pp. 285–296, 2016, doi: 10.1166/jmihi.2016.1698.

[15] D. Benitez, P. A. Gaydecki, A. Zaidi, and A. P. Fitzpatrick, "The use of the Hilbert transform in ECG signal analysis," Comput. Biol. Med., vol. 31, no. 5, pp. 399–406, 2001, doi: 10.1016/S0010-4825(01)00009-9.

[16] M. R. Homaeinezhad, A. Ghaffari, H. Najjaran Toosi, M. Tahmasebi, and M. M. Daevaeiha, "A Unified Framework for Delineation of Ambulatory Holter ECG Events via Analysis of a Multiple-Order Derivative Wavelet-Based Measure," Iran. J. Electr. Electron. Eng., vol. 7, no. 1, pp. 1–18, 2011, Accessed: May 25, 2020. [Online]. Available: http://ijeee.iust.ac.ir/article-1-238-en.html.

[17] Z. Zidelmal, A. Amirou, D. Ould-Abdeslam, A. Moukadem, and A. Dieterlen, "QRS detection using S-Transform and Shannon energy," Comput. Methods Programs Biomed., vol. 116, no. 1, pp. 1–9, 2014, doi: 10.1016/j.cmpb.2014.04.008.

[18] H. Zhu and J. Dong, "An R-peak detection method based on peaks of Shannon energy envelope," Biomed. Signal Process. Control, vol. 8, no. 5, pp. 466–474, 2013, doi: 10.1016/j.bspc.2013.01.001.

[19] H. Beyramienanlou and N. Lotfivand, "Shannon's Energy Based Algorithm in ECG Signal Processing," Comput. Math. Methods Med., vol. 2017, 2017, doi: 10.1155/2017/8081361.

[20] O. Navin, G. Kumar, N. Kumar, K. Baderia, R. Kumar, and A. Kumar, "R-peaks detection using shannon energy for HRV analysis," Lect. Notes Electr. Eng., vol. 526, pp. 401–409, 2019, doi: 10.1007/978-981-13-2553-3_39.

[21] G. B. Moody and R. G. Mark, "The impact of the MIT-BIH arrhythmia database," IEEE Eng. Med. Biol. Mag., vol. 20, no. 3, pp. 45–50, 2001, doi: 10.1109/51.932724.

[22] I. Silva and G. B. Moody, "An Open-source Toolbox for Analysing and Processing PhysioNet Databases in MATLAB and Octave," J. Open Res. Softw., vol. 2, pp. 2–5, 2014, doi: 10.5334/jors.bi.

[23] A. L. Goldberger et al., "PhysioBank, PhysioToolkit, and PhysioNet: Components of a New Reseach Resource for COmplex Physiologic Signals," Circulation, vol. 101, no. 23, 2000, doi: 10.1161/01.cir.101.23.e215.

[24] N. A. Nayan and H. A. Hamid, "Evaluation of patient electrocardiogram datasets using signal quality indexing," Bull. Electr. Eng. Informatics, vol. 8, no. 2, pp. 521–528, 2019, doi: 10.11591/eei.v8i2.1289.

[25] L. G. Tereshchenko and M. E. Josephson, "Frequency content and characteristics of ventricular conduction," J. Electrocardiol., vol. 48, no. 6, pp. 933–937, 2015, doi: 10.1016/j.jelectrocard.2015.08.034.

[26] A. A. Fedotov, A. S. Akulova, and S. A. Akulov, "Effective QRS-detector based on Hilbert transform and adaptive thresholding," IFMBE Proc., vol. 57, no. October, pp. 140–144, 2016, doi: 10.1007/978-3-319-32703-7_29.

[27] M. Elgendi, M. Jonkman, and F. Deboer, "Frequency bands effects on QRS detection," BIOSIGNALS 2010 - Proc. 3rd Int. Conf. Bio-inpsired Syst. Signal Process. Proc., no. 2002, pp. 428–431, 2010.

[28] J. E. Poole, J. P. Singh, and U. Birgersdotter-Green, "QRS duration or QRS morphology what really matters in cardiac resynchronization therapy?," J. Am. Coll. Cardiol., vol. 67, no. 9, pp. 1104–1117, 2016, doi: 10.1016/j.jacc.2015.12.039.